J Neuropathol Exp Neurol

Vol. 68, No. 8
August 2009
pp. 857–869

ORIGINAL ARTICLE

Amyloid β-Induced Nerve Growth Factor Dysmetabolism in Alzheimer Disease

Martin A. Bruno, PhD, Wanda C. Leon, Gabriela Fragoso, PhD, Walter E. Mushynski, PhD, Guillermina Almazan, PhD, and A. Claudio Cuello, MD, PhD

Abstract

We previously reported that the precursor form of nerve growth factor (pro-NGF) and not mature NGF is liberated in the CNS in an activity-dependent manner, and that its maturation and degradation occur in the extracellular space by the coordinated action of proteases. Here, we present evidence of diminished conversion of pro-NGF to its mature form and of greater NGF degradation in Alzheimer disease (AD) brain samples compared with controls. These alterations of the NGF metabolic pathway likely resulted in the increased pro-NGF levels. The pro-NGF was largely in a peroxynitrited form in the AD samples. Intrahippocampal injection of amyloid-β oligomers provoked similar upregulation of pro-NGF in naive rats that was accompanied by evidence of microglial activation (CD40), increased levels of inducible nitric oxide synthase, and increased activity of the NGF-degrading enzyme matrix metalloproteinase 9. The elevated inducible nitric oxide synthase provoked the generation of biologically inactive, peroxynitrite-modified pro-NGF in amyloid-β oligomer–injected rats. These parameters were corrected by minocycline treatment. Minocycline also diminished altered matrix metalloproteinase 9, inducible nitric oxide synthase, and microglial activation (CD40); improved cognitive behavior; and normalized pro-NGF levels in a transgenic mouse AD model. The effects of amyloid-β amyloid CNS burden on NGF metabolism may explain the paradoxical upregulation of pro-NGF in AD accompanied by atrophy of forebrain cholinergic neurons.

Key Words: Alzheimer disease, β amyloid oligomers, Minocycline, Nerve growth factor, Peroxynitrite, pro-NGF.

INTRODUCTION

Alzheimer disease (AD) is an age-related neurodegenerative disorder characterized by progressive loss of memory and deterioration of higher cognitive functions. The remarkable vulnerability of the cholinergic system to the amyloid-β (Aβ) pathology that characterizes AD is not understood. The profound loss and atrophy of basal forebrain cholinergic neurons (BFCNs) that innervate the hippocampus and the cerebral cortex contribute to the dementia-related cognitive decline and remain a main target for therapeutic intervention in AD (1).

Maintenance of the biochemical-morphological phenotype of BFCNs in adult animals is dependent on the supply of endogenous nerve growth factor (NGF) (2, 3). Furthermore, the steady state numbers of cholinergic synapses in the cerebral cortex are regulated by minute amounts of endogenous NGF (4). It would, therefore, be expected that in AD, there would be a loss of biologically active NGF. There is, however, no evidence for diminished NGF synthesis in AD (5, 6). Paradoxically, upregulation in the levels of NGF precursor protein (pro-NGF) has been well documented (7, 8). Moreover, alterations in NGF and its high-affinity receptor (TrkA) have been observed in early and late stages of AD, and increased levels of pro-NGF (7, 9) and loss of cortical TrkA (10) have been reported in subjects with mild cognitive impairment as well as in AD. The mechanism by which Aβ accumulation in AD leads to upregulation of pro-NGF with a concomitant atrophy of NGF-dependent BFCNs remains unresolved.

Recently, we gathered experimental evidence in rodents for the involvement of an extracellular protease cascade in the conversion of pro-NGF released in an activity-dependent manner to NGF and for the degradation/inactivation of NGF caused by the coordinated release and activation of matrix metalloproteinase 9 (MMP-9) (Fig. 1). We provided evidence that this mechanism is also operative in vivo because application of inhibitors of converting enzymes to the CNS led to the upregulation of brain pro-NGF levels, whereas inhibition of the degrading protease led to accumulation of mature NGF (11). We speculate that the pathway responsible for the maturation and degradation of NGF might explain the paradox of elevated pro-NGF and atrophy of NGF-dependent BFCNs in AD. Therefore, we hypothesize that Aβ accumulation in AD might provoke alterations of NGF maturation/degradation mechanisms, thereby reducing the levels of mature NGF (11); this would explain the remarkable vulnerability of FCNs in AD.

From the Departments of Pharmacology and Therapeutics (MAB, WCL, GF, GA, ACC), Biochemistry (WEM), Anatomy and Cell Biology (ACC), and Neurology and Neurosurgery (ACC), McGill University, Montreal, Quebec, Canada.

Send correspondence and reprint requests to: A. Claudio Cuello, MD, PhD, Pharmacology and Therapeutics, McGill University, 3655 Promenade Sir-William-Osler, Room 1210, Montreal, Quebec, Canada H3G 1Y6; E-mail: claudio.cuello@mcgill.ca

This work was supported by the Canadian Institute of Health Research Grant MOP 62735 and the US Alzheimer's Association IIRG-06–25861. Martin A. Bruno received a fellowship from Consejo Nacional de Investigaciones Cientıficas y Tecnicas (CONICET), Argentina, and A. Claudio Cuello holds the Charles E. Frosst Merck Chair in Pharmacology, McGill University, Montreal, Quebec, Canada.

Supplemental digital content is available for this article. Direct URL citations appear in the printed text and are provided in the HTML and PDF versions of this article on the journal's Web site (www.jneuropath.com).

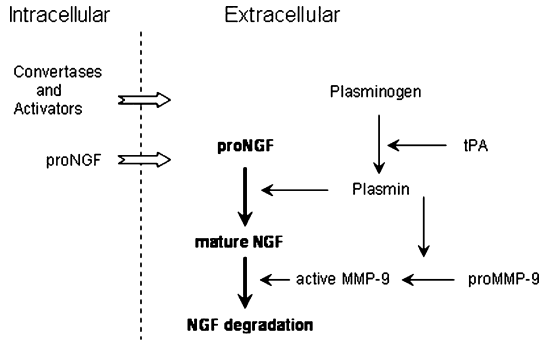

FIGURE 1. Schematic representation of the nerve growth factor (NGF) metabolic pathway. Upon stimulation, stored precursor form of NGF (pro-NGF), plasminogen, tissue plasminogen activator (tPA) and propeptide matrix metalloproteinase 9 (pro-MMP-9) are released from neurons into the extracellular space. Released tPA induces the conversion of plasminogen to plasmin. The generated plasmin converts pro-NGF into mature NGF and pro-MMP-9 into active MMP-9. Mature NGF then interacts with its cognate receptors (TrkA and p75 neurotrophin receptor) or be degraded by activated MMP-9.

Here, we investigated the status of this postulated NGF-processing pathway in AD by analyzing the components of the NGF protease cascade in human cortical tissue samples from AD and nondemented age-matched controls. We further determined whether alterations observed in AD brains also occur in a transgenic mouse model of the AD-like amyloid pathology and whether they can be experimentally replicated by the intrahippocampal injection of soluble Aβ oligomers in naive rats. In both experimental models, dysregulation of NGF metabolism was accompanied by early evidence of inflammation and peroxynitration of NGF; these abnormalities were corrected by treatment with minocycline.

MATERIALS AND METHODS

Human Brain Material

Frozen postmortem tissue samples were obtained from the Netherlands Brain Bank, Netherlands Institute for Brain Research. Clinical histories of the patients are archived at the Netherlands Brain Bank, and their demographic features are shown in the Table. This project was approved by the independent ethical committee of the Netherlands Brain Bank and by the McGill University Review Board following the Tri-Council Policy on Ethical Conduct for Research Involving Humans.

Experimental Animals

Four-month-old Fischer 344 rats were used to observe the effects of Aβ oligomers in the NGF maturation/degradation processing pathway. Two-month-old transgenic (McGill-Thy1-APP transgenic mouse model) and nontransgenic littermate mice were also used. Efforts were made to minimize the number of animals used and their suffering. All procedures were approved by the Animal Care Committee of McGill University and followed the guidelines of the Canadian Council on Animal Care.

Surgical Procedures and Hippocampal Injections

Fischer 344 rats were divided into 3 experimental groups: the first group (n = 5) was injected bilaterally into the hippocampus (following coordinates from the bregma: anteroposterior, −0.45 mm; lateral, ±0.35 mm; vertical, 0.35 mm) with 1 μg of Aβ oligomers, the second group (n = 5)

TABLE. Patient Demographics and Relative Middle Frontal Gyrus Levels of Pro-NGF, Plasminogen, tPA, and MMP-9

Age at Death, years	Sex	Right/Left Hemisphere Analyzed	Brain Weight, g	Postmortem Delay, hours	Clinical Diagnosis	Pro-NGF*	Plasminogen*	tPA*	MMP-9*
75	F	L	920	6	NCI	115	230	244	30
89	F	R	889	3	NCI	65	214	235	27
82	F	R	950	8	NCI	90	265	93	38
78	M	R	1,112	9	NCI	75	137	180	32
91	M	L	872	10	NCI	80	245	231	26
77	F	L	920	5	NCI	95	204	224	22
68	M	R	1,200	9	NCI	75	188	99	34
(80 ± 3)†			(980 ± 47)†	(7 ± 1)†	(n = 7)	(85 ± 6)†‡	(212 ± 16)†§	(186 ± 24)†§	(30 ± 2)†‖
72	M	R	1,255	7	AD	200	210	156	122
85	F	R	1,020	5	AD	170	132	63	90
88	M	L	1,460	4	AD	135	95	81	75
67	F	L	950	6	AD	154	108	54	128
74	M	L	1,350	12	AD	210	167	170	69
71	F	R	880	4	AD	122	215	58	91
88	F	R	1,050	9	AD	100	98	77	42
(78 ± 3)†			(1,138 ± 82)†	(6.7 ± 1.1)†	(n = 7)	(156 ± 15)†‡	(146 ± 19)†§	(94 ± 18)†§	(88 ± 12)†‖

*Relative middle frontal gyrus levels.
†Mean ± SEM.
‡$p < 0.01$, AD versus NCI.
§$p < 0.05$, AD versus NCI.
‖$p < 0.05$, AD versus NCI.
AD, Alzheimer disease; F, female; M, male; MMP-9, matrix metalloproteinase 9; NCI, no cognitive impairment; pro-NGF, precursor form of nerve growth factor; tPA, tissue plasminogen activator.

received bilaterally 1 μg of the reverse control peptide 42-1 (American Peptides, Sunnyvale, CA); the third group (n = 5) was treated 24 hours before the bilateral Aβ oligomer injections (1 μg) with minocycline (intraperitoneally, 50 mg/kg) (12) and daily with the same dose of minocycline (intraperitoneally) for 72 hours and then killed. Each animal was anesthetized, placed in the stereotaxic apparatus (David Kopf Instruments, Tujunga, CA), and received bilaterally a single injection of 3-μL solution containing Aβ oligomers or the 42-1 reverse control peptide diluted in phosphate-buffered artificial cerebrospinal fluid (150 mmol/L NaCl, 1.8 mmol/L $CaCl_2$, 1.2 mmol/L $MgSO_4$, 2 mmol/L K_2HPO_4, 10 mmol/L glucose, and 0.001% rat serum, pH 7.4), using a Hamilton syringe pump (flow rate, 0.25 μL/minute). The needle was left in place for 5 minutes before the injection was started; the solution was injected slowly for a period of 12 minutes. The needle was then left in place for approximately 2 to 5 minutes and retracted slowly to prevent backwash up the needle tract. After injection, the skull was swabbed, and the skin overlying the skull was closed with surgical stitches. Animals were kept alive for 72 hours and were then killed, and the hippocampus was removed and homogenized.

For intraparenchymal administration of native NGF versus peroxynitrite-modified NGF, the procedures were followed as described above, but animals (n = 5) were killed 2 hours after the injection. The doses administered (150 ng) diluted in artificial cerebrospinal fluid (final volume, 3 μL every 12 minutes) were previously shown to induce pronounced tyrosine phosphorylation of Trk-type proteins 2 hours after the injection (13).

Minocycline Pellet Implantation

Mice were anesthetized with Equithesin (composition: 1.2 g pentobarbital, 5.3 g chloral hydrate, 2.7 g $MgSO_4$.7 HO, 49.5 mL propylene glycol, 12.5 mL ethanol, and 58 mL distilled water, 0.3 mL/100 g body weight, intraperitoneally). A small incision was made in the dorsal neck region, and 1 minocycline pellet (28 day-release, 50 mg/kg per day minocycline pellet, Innovative Research, Novi, MI) or a placebo pellet (Innovative Research) was placed subcutaneously as previously described (14). The skin was then sutured with coated Vicryl (Ethicon). Animals were killed 28 days after surgery while under Equithesin anesthesia by intra-aortic perfusion with cold PBS.

Morris Water Maze Task

The animals were required to find a submerged platform in a 100-cm-diameter pool of white nontoxic colored water using only distal and spatial clues available in the testing room. Throughout the study, all tests were carried out in the same room and setup. The center of the escape platform (4.5 cm diameter) was located 25 cm from the pool wall, in the northeast quadrant. Animals were tested in 15 trials during 5 consecutive days (3 trials per day with an intertrial time of 20 minutes) with the platform 1 cm below the water. At the end of the testing periods, all animals were given 3 trials in which the platform was raised 2 cm above the water to exclude visual or motor deficits as the cause of poor performance. The swim speeds, latencies, distances, and time spent in each quadrant were recorded using a video tracking system (HVS Image, Buckinghamshire, UK). For the probe test, mice were placed in the water maze with no platform for 3 trials of 60 seconds each with an intertrial interval of 20 minutes in a single day. The data are expressed as percentage of time spent in each quadrant ±SEM, that is, the *target quadrant* being where the platform had been previously hidden.

Tissue Processing

Frozen tissues from middle frontal gyrus of nondemented (n = 7) and AD (n = 7) patients, hippocampal tissue from Fischer 344 rats, and cerebral cortex tissue from transgenic and nontransgenic mice were homogenized without thawing in 1 mL of homogenizing buffer (50 mmol/L Tris-HCl, 150 mmol/L NaCl, 1% Nonidet P-40, 0.1% sodium dodecyl sulfate, 0.1% deoxycholic acid, 2 μg/mL of aprotinin, 2 μg/mL of leupeptin, 100 μg/mL phenylmethanesulfonyl fluoride, pH 7.4). The homogenates were incubated for 15 minutes on ice and then centrifuged at 14,000 × *g* for 30 minutes at 4°C, and protein content of the supernatants was determined using the DC protein assay, as described by the manufacturer (Bio-Rad Laboratories, Hercules, CA).

Antibodies and Reagents

Antibodies from Santa Cruz Biotechnology Inc. (Santa Cruz, CA) were to: TrkA (H-190), NGF (H-20), plasminogen (H-90), tissue inhibitor of metalloproteinase 1 (H-150), MMP-9 (H-129), CD40 (C-20), tissue plasminogen activator (tPA) (H-90), and inducible nitric oxide synthetase (iNOS) (N-20). Other antibodies used were polyclonal anti–pro-NGF (Alomone Labs, Jerusalem, Israel), mouse monoclonal anti-nitrotyrosine (ab24496; Abcam Inc, Cambridge, MA), anti-phospho TrkA (Cell Signaling Technology, Beverly, MA), A11 (gift from Dr Glabe, Irvine, CA) and 6E10 monoclonal antibody (Millipore, Ontario, Canada), and monoclonal antineurofilament antibody (N52; Sigma-Aldrich, Oakville, Ontario, Canada). Secondary antibodies were from Jackson Immunoresearch Laboratories (Cedarlane, Ontario, Canada). Peroxynitrite and degraded peroxynitrite was from Upstate Biotechnology (Millipore, Billerica, MA); recombinant pro-NGF was from Alomone Labs; NGF was from Cedarlane Laboratories; plasmin was from Molecular Innovations Inc (Southfield, MI); Aβ (1–42) peptide and the reverse control peptide (42-1) were from American Peptide Company; minocycline was from Sigma-Aldrich.

Immunoprecipitation

To elute the protein with minimal antibody contamination, cross-linking of the antibodies (TrkA and NGF) to Sepharose A beads (Sigma-Aldrich, Canada) was performed following the Abcam online protocol. In brief, the Sepharose A beads were washed in 1 mL PBS–bovine serum albumin 1% wt/vol mix for 1 hour and rinsed in PBS twice. The supernatant was removed, and 400 μL of homogenizing buffer containing protease inhibitors was added. For each sample, 100 μL of beads were incubated with 300 μg of total protein of brain homogenates overnight at 4°C under agitation. After washing the beads 3 times with homogenizing buffer at 4°C, loading buffer was added, and this was boiled at 95°C to

100°C for 5 minutes to denature the protein and separate it from the protein-A beads. The samples were then centrifuged, and the supernatant was loaded and resolved by sodium dodecyl sulfate-polyacrylamide gel electrophoresis.

Western Blot Analysis

Forty to 100 μg of total protein of each sample was separated on 8% to 12% polyacrylamide resolving gels. Proteins were then transferred onto nitrocellulose membranes and blocked 1 to 2 hours at room temperature (RT) in TBS-T (Tris buffer, 10% Tween-20) with 5% (wt/vol) nonfat milk powder (Carnation). Incubations with primary antibodies were performed overnight at 4°C. After washing, membranes were incubated with horseradish peroxidase-conjugated secondary antibodies for 1 hour at RT. For detection, an enhanced chemiluminescence system (GE Healthcare Life Sciences, NJ) was used according to the manufacturer's instructions. The immunoreactive bands were quantified by densitometry of the films using MCID image analysis system. Values were normalized to β-III tubulin.

Gelatin Zymography

Sixty micrograms of each sample was resolved on 10% polyacrylamide gels containing 0.1% gelatin. After electrophoresis, the gel was incubated in zymogram renaturing buffer (Triton X-100, 25% [vol/vol] in water) with gentle agitation during 30 minutes at RT. After decanting the zymogram renaturing buffer, gels were incubated overnight at 37°C with gentle agitation in developing buffer (50 mmol/L Tris-HCl, 0.2 mol/L NaCl, 5 mmol/L $CaCl_2$, 0.02% Brij 35, pH 7.6). The gels were then stained with Coomassie blue R-250 (0.5% in ethanol 40%) for 30 minutes. Areas of protease activity appeared as clear bands against a dark blue background after incubation of the gel with an appropriate destaining solution, methanol-acetic acid-water (40:10:50).

Aβ Oligomer Preparation

Amyloid-β oligomers were prepared as described by Demuro et al (15). Briefly, soluble Aβ oligomers were prepared by dissolving 1.0 mg of peptide in 400 μL of hexafluoroisopropanol at RT. Then, 100 μL of the resulting seedless solution was added to 900 μL double-distilled water and centrifuged for 15 minutes at 14,000 × *g*, and the supernatant fraction was transferred to a new tube and subjected to a gentle stream of N_2 for 5 to 10 minutes to evaporate the hexafluoroisopropanol. Finally, the samples were stirred at 500 rpm using a Teflon-coated microstir bar for 24 to 48 hours at 22°C. The final peptide concentration was 1 μg/μL. The reverse control peptide (42-1) followed the same processing.

Dot Blot Analysis

Using a narrow-mouth pipette, 2 μL of fresh monomeric Aβ peptide and 2 μL of soluble Aβ oligomeric solution were spotted onto the nitrocellulose membrane. After drying, the membrane was soaked in 5% bovine serum albumin in TBS-T for 1 hour at RT to block nonspecific sites. The membrane was then incubated with different primary antibodies (A11 and 6E10 diluted 1:1000 in bovine serum albumin/TBS-T) for 1 hour at RT. The membrane was washed (3 × 5 minutes) with TBS-T and incubated with the corresponding secondary antibody conjugated with horseradish peroxidase (1:10,000) for 30 minutes at RT. After washing (3 × 5 minutes), the membrane was incubated with enhanced chemiluminescence reagent for 1 minute and exposed to x-ray film in the dark room.

Peroxynitrite-Modified NGF and Pro-NGF Preparations

Nerve growth factor (1 μg) or recombinant pro-NGF (1 μg) was treated with peroxynitrite in 50 mmol/L sodium phosphate buffer and 20 mmol/L sodium bicarbonate, pH 7.4, following the protocol described by Pehar et al (16). At the time of the experiment, peroxynitrite concentration (by absorbance at 302 nm) was ε = 1,690 M^{-1} $^{cm-1}$. Fresh stock solutions were prepared in 0.01 mol/L NaOH, and the reaction was performed at 37°C. Peroxynitrite was added to the top of the tube (containing NGF or pro-NGF) 5 times and mixed by vortexing for 3 seconds to reach the final peroxynitrite concentration of 1 mmol/L. The same procedures were applied for decomposed peroxynitrite (reverse-order addition) diluted in 0.001 mol/L NaOH.

Statistical Analysis

Statistical significance between pixel values for control and AD groups was calculated using the *t*-test; bars represent the mean intensities ±SEM for each group. Behavioral data were subjected to univariate and multivariate analysis of variance. For repeated measures, the Huynh-Feldt p value is reported. Between-group comparisons were made using Tukey test. All probabilities were 2-tailed; a level of 5% was considered significant.

RESULTS

Altered NGF Maturation and Cortical Pro-NGF Accumulation in AD Brain

In the AD samples, there were greater levels of pro-NGF (32 kd band, $p < 0.01$; Fig. 2A), decreased levels of plasminogen ($p < 0.05$; Fig. 2B) and tPA ($p < 0.05$), and a correspondently significant decrease in the formation of plasmin ($p < 0.001$; Figs. 2B, C; Table) compared with controls; plasmin ultimately converts pro-NGF into mature NGF (11, 17). These results indicate that there is a marked deficit in the cascade responsible for NGF maturation in AD. This failure in pro-NGF conversion would explain the progressive accumulation of pro-NGF in AD cerebral cortex in the presence of normal NGF mRNA levels (5, 6).

Increased NGF Degradation Activity in AD

Greater levels of MMP-9 have been identified in AD than in age-matched control samples of hippocampal tissue (18) and plasma (19). We confirmed increased levels and activity of MMP-9 in cortical human AD brain tissue as assessed by Western blot analysis ($p < 0.001$; Fig. 2D; Table) and gelatin zymography ($p < 0.001$; Fig. 2D), respectively. Moreover, no significant changes in the tissue inhibitor of MMP-9, tissue inhibitor of metalloproteinase 1, were observed in AD cortical tissue compared with age-matched controls ($p > 0.05$; Fig. 2E).

Matrix metalloproteinase 9 is released in an activity-dependent manner as a propeptide (pro-MMP-9) that can be

then activated by plasmin (11), but we found increased pro-MMP-9 and MMP-9 levels in cortical AD samples, strongly suggesting an alternative mechanism for MMP-9 activation because the tPA/plasminogen/plasmin system is downregulated in AD. Because S-nitrosylation of pro-MMP-9 by NO has been described as an alternative mechanism for activation of MMP-9 in response to oxidative stresses (20) and Aβ directly induces the expression of MMP-9 (21), we investigated whether NO production participates in this NGF metabolic dysregulation in AD brains.

Microglia Activation and NO Production in AD

Activation of microglia by aggregated Aβ is a central feature in the chronic inflammatory pathology in AD (22) anda direct indicator of an ongoing chronic inflammatory process. Nitric oxide is synthesized by a family of enzymes named NOS, including iNOS, endothelial NOS, and neuronal NOS. Inducible NOS is found in activated microglia, whereas NO production (23) and neuronal expression of iNOS are also found in AD brains (24, 25). We investigated the levels of activated microglia and iNOS expression in cortical AD tissue and compared these with age-matched controls. CD40 expression is a well-established marker of microglial activation, which is upregulated in the presence of Aβ peptides (26, 27). CD40 is also upregulated by activated microglia in AD brains (28, 29). Consistent with these previous reports, we found increased levels of both CD40 ($p < 0.001$; see Supplemental Fig. 1A, Supplemental Digital Content 1, http://links.lww.com/A1399) and iNOS ($p < 0.05$; see Supplemental Fig. 1B, Supplemental Digital Content 1, http://links.lww.com/A1399). These results indicate the occurrence of microglial activation and increased NO production

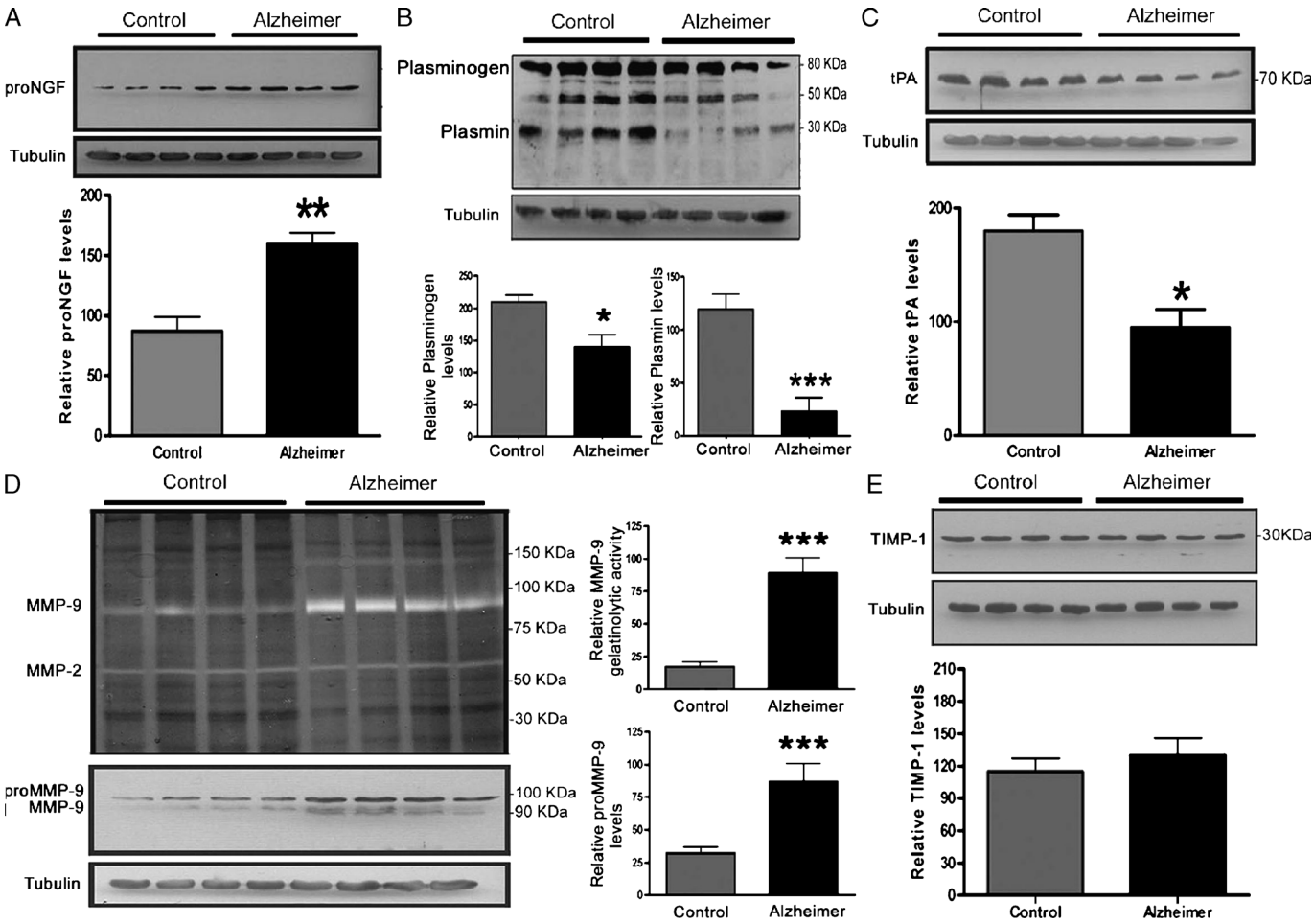

FIGURE 2. Altered cortical levels of the nerve growth factor (NGF) maturation/degradation cascade components in Alzheimer disease. Western blot analysis from middle frontal gyrus of Alzheimer disease (AD) brain homogenates compared with age-matched controls reveals: **(A)** increased amounts of precursor form of NGF ([pro-NGF] 32 kd band, $p < 0.01$), **(B)** decreased levels of plasminogen ($p < 0.05$) and plasmin ($p < 0.001$), and **(C)** decreased levels of tissue plasminogen activator ([tPA] $p < 0.05$). **(D)** The upper panel illustrates the increased matrix metalloproteinase 9 (MMP-9) gelatinolytic activity in the middle frontal gyrus of AD versus control samples by gelatin zymography ($p < 0.001$). In the lower panel, increased pro-MMP-9 and active MMP-9 levels were found in AD by Western blot ($p < 0.001$). **(E)** No significant differences were found by Western blot analysis of the MMP-9 inhibitor tissue inhibitor of metalloproteinase 1 (TIMP-1) in the middle frontal gyrus of AD samples compared with age-matched controls ($p > 0.05$). Quantification of the immunoreactive bands was determined by densitometry of the films using MCID program, and pixel values were normalized to β-III tubulin values for each sample ($n = 7$ for each group).

in AD brains. The increased brain content of NO would facilitate the observed hyperactivity of MMP-9 in AD, thereby diminishing the availability of biologically active NGF. Based on the above observations, we performed further studies to determine whether microglial activation and increased NO production could be triggered by Aβ-oligomers in vivo.

In Vivo Effects of Injected Soluble Aβ Oligomers on Pro-NGF Levels and MMP-9 Activity

Brain levels of soluble Aβ in AD show a stronger correlation with cognitive impairments than plaque density (30–32). Consequently, our next step was to investigate whether the altered expression of pro-NGF, MMP-9, CD40,

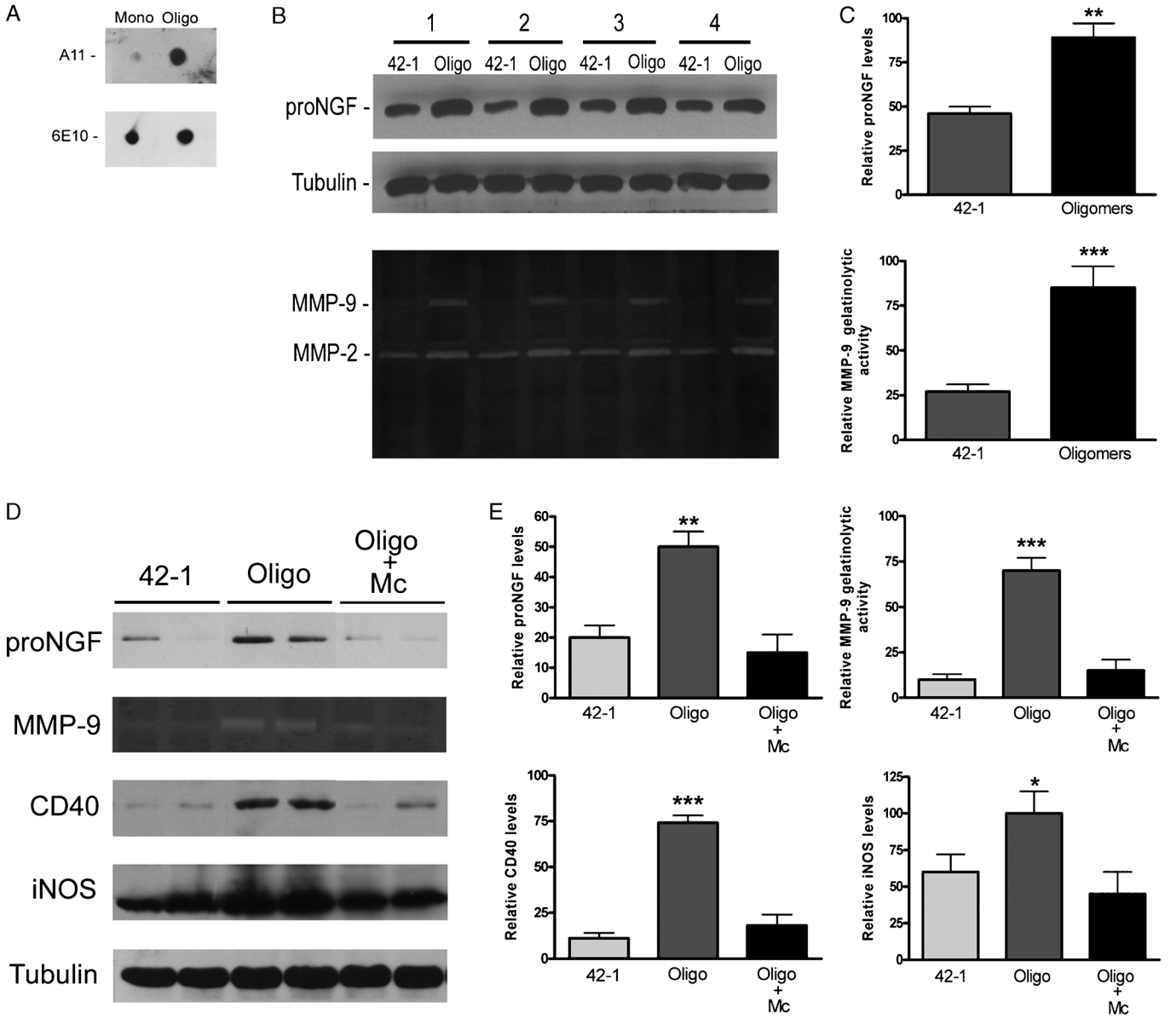

FIGURE 3. In vivo effects of soluble amyloid β (Aβ) oligomers in the nerve growth factor (NGF) maturation/degradation cascade. **(A)** Before hippocampal injections, the formation of soluble Aβ oligomers were confirmed by dot blot analysis using the A11 antibody that recognizes the presence of oligomers and the 6E10 antibody that recognizes monomers and oligomeric forms of Aβ. **(B)** Seventy-two hours after Aβ oligomers (Oligo) or reverse peptide (42-1) were injected into the hippocampus, levels of precursor form of NGF (pro-NGF) were determined by Western blot and matrix metalloproteinase 9 (MMP-9) activity was analyzed by gelatin zymography. Note the upregulation of pro-NGF levels and of MMP-9 activity in hippocampi receiving Aβ oligomers. **(C)** Histogram representation of the relative values of pro-NGF and MMP-9 activity. Quantification of bands was performed by densitometry using MCID program; values were normalized to β-III tubulin for Western blots (pro-NGF) and to MMP-2 for zymograms (MPP-9 activity). Statistical differences ** ($p < 0.01$) and *** ($p < 0.001$) were found in Aβ oligomers-injected side samples compared with the control 42-1 reverse peptide-injected side samples ($n = 5$). **(D, E)** Minocycline (Mc) treatment ($n = 5$) prevented the increase in pro-NGF ($p < 0.01$), MMP-9 ($p < 0.001$), microglia activation (CD40; $p < 0.001$), and inducible nitric oxide synthetase ([iNOS] $p < 0.05$) upregulation induced by Aβ oligomers.

and iNOS observed in AD brains could be triggered by neurotoxic Aβ oligomers (33). We administered a single injection of soluble Aβ oligomers (ipsilateral, 1 μg/3 μL) versus the reverse peptide 42-1 as control (contralateral, 1 μg/3μL) in the rat hippocampus for 72 hours. Soluble Aβ oligomers were prepared as previously described (15), and the Aβ oligomerization was confirmed by dot blot analysis, applying the oligomeric peptide-specific A11 antibody (34) and 6E10 antibody using the monomeric peptide form as control (Fig. 3A). In Aβ oligomer-injected hippocampi, we found increased levels of pro-NGF ($p < 0.01$) and of MMP-9 activity ($p < 0.001$) compared with the reverse peptide-injected contralateral hippocampi (Figs. 3B, C). Moreover, tPA levels were markedly decreased in the Aβ oligomers-injected side compared with the reverse peptide-injected side (data not shown).

Minocycline Prevented the Aβ Oligomer-Induced Alterations in the NGF Maturation/Degradation Cascade and in Microglial Activation

These observations led us to speculate that targeting microglial activation to prevent iNOS expression and NO production in AD could correct the increased pro-NGF levels and/or the MMP-9 hyperactivation, along with preventing microglial activation. To test this, rats infused with soluble Aβ oligomers were treated with minocycline, a tetracycline derivative that has been shown to attenuate microglial activation by decreasing the production of proinflammatory molecules (35), lowering iNOS expression (36, 37) and inhibiting MMP-9 (12). Minocycline was administered 24 hours before soluble Aβ oligomers were injected and daily afterward for 72 hours; animals were then killed, and hippocampal tissue was processed for neurochemical analysis. Minocycline-treated animals infused with Aβ oligomers were significantly protected from the Aβ-induced upregulation of pro-NGF ($p < 0.01$) and of MMP-9 ($p < 0.001$) as well as the elevation of microglial CD40 ($p < 0.001$) and of iNOS ($p < 0.05$) expression compared with Aβ oligomer-infused rats not treated with minocycline (Figs. 3D, E). No statistically significant differences were found between minocycline-treated rats injected with soluble Aβ oligomers and rats injected only with 42-1 reverse control peptide.

Peroxynitrite-Mediated Nitrotyrosine Formation in Pro-NGF and NGF

We next investigated whether increased NO production could impact the degree of pro-NGF–peroxynitration or on NGF activity. Nitrotyrosine immunoreactivity has been shown to be 5- to 8-fold higher in areas of neurodegeneration in AD brain than in cognitively normal subjects (25, 38, 39). In agreement with these findings, we observed a clear increment in the content and number of nitrotyrosine-immunoreactive bands in AD brain samples compared with age-matched controls (Fig. 4A).

We further investigated whether the increased cortical pro-NGF seen in AD also contains nitrotyrosine residues. Material immunoprecipitated with anti-NGF and resolved by Western blot was found to contain a high-molecular band (32kd) corresponding to pro-NGF (Fig. 4B), the predominant form of NGF in the human (7) and rodent brain (11). Equally loaded immunoprecipitated material resolved by Western blot was probed with an antibody against nitrotyrosine, demonstrating the presence of nitrotyrosine-positive bands in AD brain samples and almost undetectable levels of nitrated pro-NGF in age-matched controls (Fig. 4C). These results indicated that there is a clear accumulation of peroxynitrite-modified pro-NGF in cortical tissue of AD brain.

As shown in Figure 3D, a single injection of soluble Aβ oligomers into the rat hippocampus increased levels of iNOS after 72 hours. To test the possibility that under such conditions peroxynitration of protein does occur, the brain homogenates were further resolved by Western blot analysis using the nitrotyrosine antibody. As expected, additional nitrotyrosine-positive bands appeared in the samples injected with Aβ oligomers compared with the control samples injected with 42-1 reverse peptide. Moreover, this peroxynitrite-mediated oxidative damage could be prevented by treatment with minocycline (Fig. 4D). To investigate whether soluble Aβ oligomers are specifically able to induce the nitration of tyrosine residues in pro-NGF/NGF molecules, these proteins were immunoprecipitated with NGF antibodies. This revealed an accumulation of nitrated pro-NGF in the samples injected with soluble Aβ oligomers; this was also prevented by minocycline treatment (Fig. 4E).

To understand whether the pro-NGF accumulation observed in AD cortical tissue could be induced by the peroxynitrite-mediated oxidation of pro-NGF, recombinant purified recombinant pro-NGF (32 kd) and mature NGF (14 kd) were treated with peroxynitrite ($ONOO^-$, 1 mmol/L) as previously described (16). The reaction products were resolved by Western blot analysis using anti-NGF (Fig. 4F) and antinitrotyrosine antibodies (Fig. 4G). Mature NGF (Lane 1) and pro-NGF (Lane 4) were also treated with decomposed peroxynitrite (1 mmol/L, Lines 2 and 5, respectively) as controls. No differences were observed after decomposed peroxynitrite treatment compared with untreated mature NGF and recombinant pro-NGF. After peroxynitrite treatment, however, nitrotyrosine-positive bands were observed for both NGF and pro-NGF (Lanes 3 and 6, respectively). In addition, we tested whether plasmin was capable of maturing peroxynitrite-modified pro-NGF. In Figure 4F Lane 7, 2 NGF-positive bands corresponding to pro-NGF and mature NGF can be seen; these indicate that plasmin was able to convert peroxynitrite-modified pro-NGF into nitrotyrosine-containing mature NGF. After plasmin treatment, this reactive product was resolved using a nitrotyrosine antibody; a 14-kd band corresponding to mature NGF was observed (Fig. 4G, Line 7). This result indicates that peroxynitrite-modified pro-NGF is converted by plasmin into nitrated mature NGF.

Altered Capacity of Peroxynitrite-Modified NGF to Induce Phosphorylation of TrkA In Vivo

To investigate whether the lack of trophic support of oxidized NGF displayed in vitro with cultured dorsal root ganglion neurons (see Supplemental Fig. 2, Supplemental

Digital Content 2, http://links.lww.com/A1400) is also seen in vivo, we injected native NGF and peroxynitrite-modified NGF unilaterally into the rat hippocampus. At 2 hours after the injections, we determined the levels of TrkA autophosphorylation in the hippocampus. After immunoprecipitation using an anti-TrkA antibody, Western blots of phosphorylated TrkA and total TrkA (Fig. 4H) revealed a significant reduction in the level of TrkA phosphorylation ($p < 0.001$) on the side injected with peroxynitrite-modified NGF compared with the side injected with native NGF. These results indicate that peroxynitrite modifies NGF activity, resulting in a reduced ability to induce TrkA autophosphorylation and, therefore, disrupting the first steps in the NGF signaling cascade.

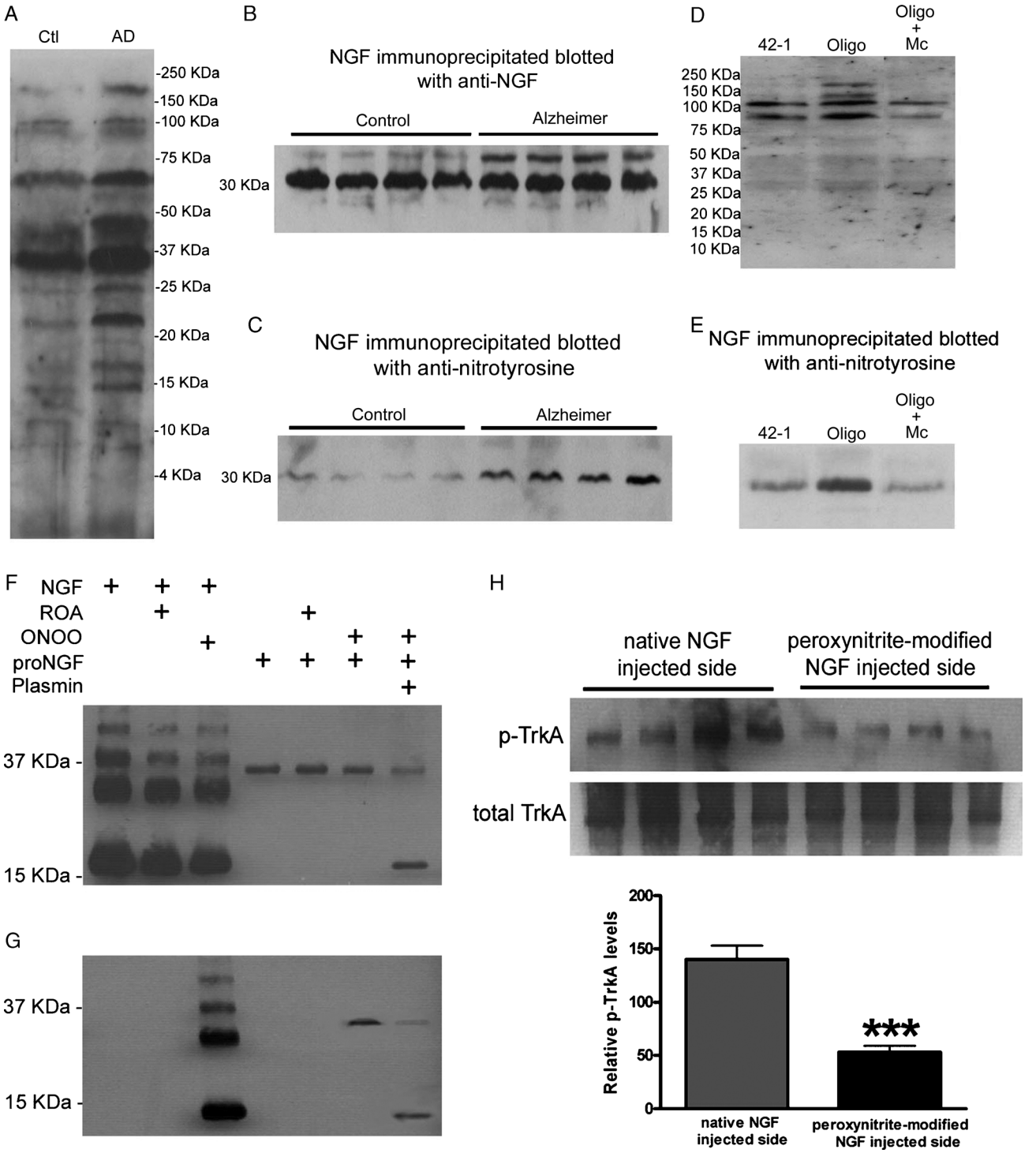

Minocycline Treatment of the McGill-Thy1-APP Transgenic Mouse Model Prevented Alterations on the NGF Maturation/Degradation Cascade and Ameliorated Behavioral Deficits

We further investigated whether the modifications in content and nitration of pro-NGF/NGF observed in AD brain samples and in rats infused with soluble Aβ oligomers were also present in the McGill-Thy1-APP transgenic mouse model (see Supplemental Fig. 3A, Supplemental Digital Content 3, http://links.lww.com/A1401). The observed behavioral impairment at 3 months of age in these mice (see Supplemental Fig. 3B, Supplemental Digital Content 3, http://links.lww.com/A1401) was coincident with increased cortical pro-NGF ($p < 0.05$) and iNOS ($p < 0.05$) content and altered MMP-9 activity ($p < 0.05$) (see Supplemental Fig. 3B, Supplemental Digital Content 3, http://links.lww.com/A1401). We administered minocycline to these mice daily for 28 days, starting 1 month before the appearance of cognitive deficits and dysregulation of the NGF processing pathway. Transgenic mice ($n = 8$) received a dose of minocycline in pellet formulation previously shown to be neuroprotective (50 mg/kg per day) (14), whereas a transgenic mouse control group ($n = 8$) received placebo pellets. As controls, we also included 2 groups of littermate nontransgenic mice given placebo ($n = 8$) or minocycline ($n = 7$) pellets. At the end of the treatment, the animals were tested for their ability to learn the Morris water maze task, as previously described (40). There were no differences in performance between placebo and minocycline nontransgenic control groups in the acquisition of the Morris water maze task (Fig. 5A). On the other hand, the performance of the transgenic placebo-treated group differed from those of the nontransgenic placebo-treated littermates ($p < 0.0001$, $F_{4,60} = 36.70$) and the minocycline-treated transgenic group ($p < 0.0001$, $F_{4,60} = 13.40$). There were no statistically significant differences in performance between the nontransgenic littermates and the minocycline-treated transgenic group ($p > 0.02$, $F = 3.09$) (Fig. 5A). The quadrant analysis performed during the probe test 24 hours after the end of the acquisition phase (Fig. 5B) revealed that placebo-treated transgenic mice spent significantly less time (as a percentage) in the quadrant where the platform was located as compared with the other treated groups ($p < 0.001$).

Biochemical analysis of inflammatory markers and pro-NGF in minocycline-treated transgenic animals showed normalization of cortical pro-NGF and iNOS levels as well as of MMP-9 activity (Fig. 5C). As shown in Figure 5D, transgenic mice receiving placebo treatment displayed increased pro-NGF levels ($p < 0.01$) analogous to that observed in AD, whereas the level of pro-NGF in minocycline-treated mice statistically did not differ from the levels found in non-transgenic littermates ($p > 0.05$). When the cortical NGF from minocycline-treated mice was immunoprecipitated and blotted with antinitrotyrosine antibody, the content of peroxynitrite-modified pro-NGF was found to be markedly reduced (Fig. 5C). Furthermore, minocycline treatment also normalized the MMP-9 activity ($p < 0.01$) and reduced the altered levels of iNOS ($p < 0.05$) observed in transgenic mice treated with placebo (Figs. 5E, F, respectively).

DISCUSSION

We found a marked alteration in the level of the protease cascade responsible for NGF maturation in human AD cortical tissue. Diminished plasmin formation in AD brain would reduce the NGF maturation process, resulting in the accumulation of pro-NGF. In addition, we found increased levels of MMP-9 and of its proteolytic activity in AD cortical tissue. This protease can rapidly degrade mature NGF, but it does not convert pro-NGF into mature NGF (11). The combination of diminished conversion to mature biologically active NGF along with the increased levels and activity of the NGF-degrading

FIGURE 4. Peroxynitration of precursor form of nerve growth factor (pro-NGF) and NGF in Alzheimer disease (AD). **(A)** Representative Western blots showing the high proportion of nitrotyrosine protein contents in middle frontal gyrus of AD samples and age-matched controls (Ctl) using a monoclonal antinitrotyrosine antibody. **(B)** Three hundred micrograms of total protein from middle frontal gyrus homogenates from AD and controls were immunoprecipitated with NGF antibody and resolved by Western blot and further **(C)** blotted with the monoclonal antinitrotyrosine antibody, revealing a marked tyrosine nitration of pro-NGF (32 kd) molecules in AD brain samples. **(D)** Sixty micrograms of hippocampal homogenates from rats injected with 42-1 reverse control peptide, soluble amyloid β (Aβ) oligomers (Oligo), and minocycline (Mc)-treated rats also injected with soluble Aβ oligomers (5 animals per condition) were separated and blotted with antinitrotyrosine antibody. Additional nitrotyrosine-positive bands are seen in Aβ-injected rats. The Mc treatment markedly diminished the nitrotyrosine modifications of proteins in Aβ oligomer-treated samples. **(E)** Hippocampal homogenates from injected rats were immunoprecipitated with NGF antibody, separated, and blotted with antinitrotyrosine antibody, showing that Aβ oligomers caused nitration of tyrosine residues in pro-NGF, which was prevented by Mc treatment. **(F)** Representative Western blot showing the effects of peroxynitrite ($ONOO^-$, 1 mmol/L) on mature NGF (10 ng/well) and recombinant pro-NGF (50 ng/well): NGF (Lane 1), NGF treated with decomposed peroxynitrite (1 mmol/L) (reverse-order addition [ROA] decomposed peroxynitrite) (Lane 2), NGF treated with peroxynitrite (Lane 3), pro-NGF (Lane 4), pro-NGF treated with ROA (Lane 5), pro-NGF treated with peroxynitrite (Lane 6), and pro-NGF treated with peroxynitrite and plasmin (2 μg/μL) (Lane 7). The final reaction products were separated by sodium dodecyl sulfate-polyacrylamide gel electrophoresis and blotted with anti-NGF antibody. **(G)** The same reaction products were immunoblotted with antinitrotyrosine antibody revealing the presence on peroxynitrite-modified NGF (Lane 3), peroxynitrite-modified pro-NGF (Lane 6), and peroxynitrite-modified mature NGF derived from peroxynitrite-modified pro-NGF and converted (matured) by the action of plasmin (Lane 7). **(H)** Reduced capacity of peroxynitrite-modified NGF to induce TrkA phosphorylation in vivo. A total of 150 ng of native NGF or peroxynitrite-modified NGF were injected into the rat hippocampus, and 2 hours later, the animals where killed, and the tissue was subjected to immunoprecipitation with TrkA antibody and separated by Western blot. When compared with the side injected with native NGF, peroxynitrite-modified NGF displayed a significant reduction in its capacity to induce TrkA phosphorylation ($n = 5$; $p < 0.001$).

protease MMP-9 creates a situation of double jeopardy for the trophic support of BFCNs in AD brain. It is, thus, plausible that alterations in the balance of NGF maturation and degradation may be the cause of abnormally elevated pro-NGF in AD and that this could provoke or contribute to the remarkable vulnerability of the NGF-dependent forebrain cholinergic

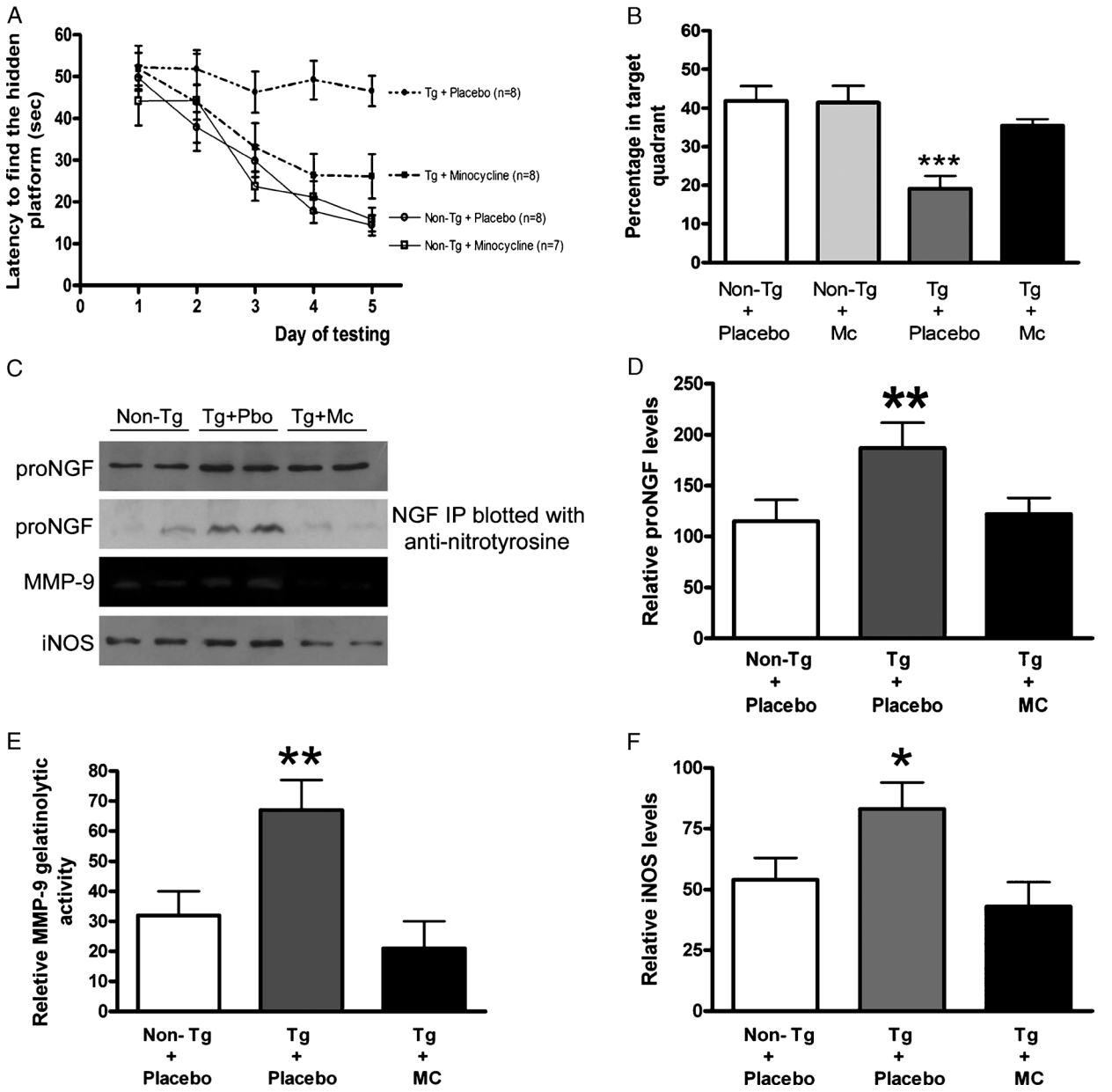

FIGURE 5. Minocycline (Mc) prevents nerve growth factor (NGF) maturation/degradation alteration and corrects behavioral deficits in McGill-Thy1-APP transgenic (Tg) mice. **(A)** Minocycline treatment for 28 days reversed the behavioral impairment displayed by 3-month-old Tg mice. The Tg placebo (Pbo)-treated group performed poorly in the learning of the Morris water maze task and differed from the Pbo non-Tg littermates group ($p < 0.0001$, $F = 36.70$) and from the Tg Mc-treated group ($p < 0.0001$, $F = 13.40$). There was no statistical difference between the Mc-treated and Pbo-treated non-Tg littermates compared with the Mc-treated Tg group ($p > 0.02$ and $p > 0.05$, respectively, $F = 3.09$). **(B)** The quadrant analysis performed during the probe test 24 hours after the end on the acquisition phase revealed that Tg Pbo mice spent significantly less time (as percentage) in the trained quadrant (where the platform was located) compared with the other treated groups ($p < 0.001$). **(C)** Increased precursor form of NGF (pro-NGF) levels were observed in Tg Pbo mice (**D**; $p < 0.01$, $n = 8$); the level of pro-NGF in Mc Tg mice ($n = 8$) did not statistically differ from the levels found in non-Tg littermates ($p > 0.05$, $n = 8$). Cortical NGF molecular forms were immunoprecipitated and blotted with antinitrotyrosine antibody. Abundant peroxynitrated pro-NGF was found in Pbo Tg mice, whereas the content of peroxynitrite-modified pro-NGF was dramatically reduced in Mc Tg mice. Minocycline also normalized the matrix metalloproteinase 9 (MMP-9) activity (**E**, $p < 0.01$, $n = 8$) and reduced the altered levels of inducible nitric oxide synthetase ([iNOS] **F**, $p < 0.05$, $n = 8$) observed in Tg Pbo mice.

neurons in AD. This hypothesis requires further experimental investigation.

Current evidence supports the view that soluble β amyloid peptides induce impairments of memory formation (41–43), a mechanism that probably involves the basal forebrain cholinergic system (44, 45). We investigated whether the observed impaired processing of pro-NGF and the increased degradation of NGF was directly linked to the occurrence of neurotoxic Aβ oligomers in the brain. Our observations support the notion that the presence of Aβ oligomers in the brain is sufficient to induce the elevation of pro-NGF levels and the synthesis and activation of MMP-9.

There is increasing evidence indicating that oxidative damage to proteins and other macromolecules is a salient feature of AD pathology (25, 39, 46–48). Microglial cells are normally in a resting state, but in AD, they gradually become activated with simultaneous production of superoxide and NO (23, 39). In vitro studies have shown that activated microglia become neurotoxic through generation of peroxynitrite, a powerful oxidant molecule formed by the reaction of superoxide with NO (49–51). Peroxynitrite is a potent oxidant and nitrating agent involved in the oxidation and nitration of tyrosine residues in proteins (47, 52). Our observations in AD brain, in studies involving delivery of soluble Aβ oligomers into rat hippocampus and in transgenic mice, reinforce the concept that microglial activation leading to iNOS production would result in peroxynitrite-mediated nitration of key metabolic proteins, including neurotrophins. Moreover, there is now considerable evidence that inflammatory stimuli induce the expression of iNOS mRNA, protein, and enzymatic activity in neuronal populations in AD (53). However, regardless of its origin (glial or neuronal), NO is a soluble diffusible gas that may act on neighboring cells by forming peroxynitrite and thus nitrating key proteins. This situation might signal the involvement of an added factor in the pathogenesis of neurodegeneration in AD because it has been shown that peroxynitrite converts NGF into proapoptotic factor in motor neurons (16). Other investigators have, however, proposed that motor neuron cell death is mediated by peroxynitrite-induced release of pro-NGF instead of NGF (54).

Cortical accumulation of pro-NGF might favor atrophy or cell death of NGF-dependent neurons as it binds with high affinity to $p75^{NTR}$ but does not bind to the TrkA receptor (55). Because we found high levels of peroxynitrite-modified pro-NGF in AD brain that could be partially converted to peroxynitrited NGF, we investigated whether this molecular form can sustain biologic responses in TrkA-expressing neurons. We observed that nitrated NGF loses biologic activity, as reflected by the poor survival of newly cultured dorsal root ganglion neurons or a diminished neuronal phenotype of mature and fully differentiated dorsal root ganglion cultures. Such molecular modifications would have a further negative impact in the trophic support of NGF-dependent neurons in the context of AD. Our in vivo experiments of injecting peroxynitrated NGF into the hippocampus would further reinforce this concept. The present findings add a new perspective to the poorly understood vulnerability of BFCNs in AD. The well-noted reduction of TrkA proteins in AD (10) would be in line with the present findings of perturbed NGF maturation and increased degradation and peroxynitration of NGF. It would also concur with the well-established notion that TrkA gene expression is induced by biologically active mature NGF (56–58).

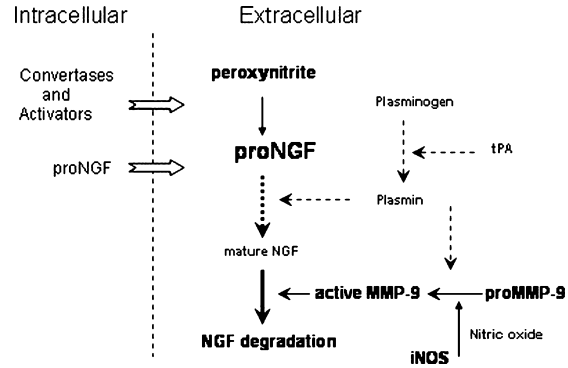

FIGURE 6. Schematic representation of the disruption in the nerve growth factor (NGF) maturation/degradation pathway. Amyloid β-induced microglial activation would generate inducible nitric oxide synthetase (iNOS) expression, NO production, peroxynitrite formation, increased matrix metalloproteinase 9 (MMP-9) activity, thus altering NGF maturation/degradation pathway and NGF peroxynitration, ultimately leading to the trophic disconnection of basal forebrain cholinergic neurons. MMP-9, matrix metalloproteinase 9; tPA, tissue plasminogen activator.

In summary, our results suggest that Aβ-induced AD pathology involves a profound alteration in the maturation, degradation, and degree of peroxynitration of NGF. This scenario would result in a drastic reduction of the biologic actions of NGF needed for the phenotypic maintenance of the NGF-dependent BFCNs as a consequence of the Aβ burden in AD. Our findings also suggest that some of the alterations in NGF metabolism are generated by Aβ-induced microglial activation. Based on the present results, Figure 6 summarizes the proposed alterations of the NGF metabolism in AD.

ACKNOWLEDGMENTS

The authors wish to dedicate this communication to Rita Levi-Montalcini, discover of NGF, on her 100TH birthday.

The authors thank Adriana Ducatenzeiler and Vanessa Partridge for excellent technical support and Mona-Lisa Bolduc for editorial assistance. The authors would also like to thank Charles Glabe (Irvine, CA) for the generous provision of A11 antibodies.

REFERENCES

1. Giacobini E, Becker RE. One hundred years after the discovery of Alzheimer's disease. A turning point for therapy? J Alzheimers Dis 2007;12:37–52
2. Cuello AC. Effects of trophic factors on the CNS cholinergic phenotype. Prog Brain Res 1996;109:347–58
3. Thoenen H. Neurotrophins and neuronal plasticity. Science 1995;270: 593–98
4. Debeir T, Saragovi HU, Cuello AC. A nerve growth factor mimetic TrkA antagonist causes withdrawal of cortical cholinergic boutons in the adult rat. Proc Natl Acad Sci U S A 1999;96:4067–72

5. Fahnestock M, Scott SA, Jette N, et al. Nerve growth factor mRNA and protein levels measured in the same tissue from normal and Alzheimer's disease parietal cortex. Brain Res Mol Brain Res 1996;42:175–78
6. Jette N, Cole MS, Fahnestock M. NGF mRNA is not decreased in frontal cortex from Alzheimer's disease patients. Brain Res Mol Brain Res 1994;25:242–50
7. Fahnestock M, Michalski B, Xu B, et al. The precursor pro-nerve growth factor is the predominant form of nerve growth factor in brain and is increased in Alzheimer's disease. Mol Cell Neurosci 2001;18:210–20
8. Peng S, Wuu J, Mufson EJ, et al. Increased proNGF levels in subjects with mild cognitive impairment and mild Alzheimer disease. J Neuropathol Exp Neurol 2004;63:641–49
9. Peng S, Wuu J, Mufson EJ, Fahnestock M. Precursor form of brain-derived neurotrophic factor and mature brain-derived neurotrophic factor are decreased in the pre-clinical stages of Alzheimer's disease. J Neurochem 2005;93:1412–21
10. Counts SE, Mufson EJ. The role of nerve growth factor receptors in cholinergic basal forebrain degeneration in prodromal Alzheimer disease. J Neuropathol Exp Neurol 2005;64:263–72
11. Bruno MA, Cuello AC. Activity-dependent release of precursor nerve growth factor, conversion to mature nerve growth factor, and its degradation by a protease cascade. Proc Natl Acad Sci U S A 2006; 103:6735–40
12. Lee CZ, Yao JS, Huang Y, et al. Dose-response effect of tetracyclines on cerebral matrix metalloproteinase-9 after vascular endothelial growth factor hyperstimulation. J Cereb Blood Flow Metab 2006;26:1157–64
13. Venero JL, Hefti F, Knusel B. Trophic effect of exogenous nerve growth factor on rat striatal cholinergic neurons: Comparison between intraparenchymal and intraventricular administration. Mol Pharmacol 1996; 49:303–10
14. Hunter CL, Bachman D, Granholm AC. Minocycline prevents cholinergic loss in a mouse model of Down's syndrome. Ann Neurol 2004; 56:675–88
15. Demuro A, Mina E, Kayed R, et al. Calcium dysregulation and membrane disruption as a ubiquitous neurotoxic mechanism of soluble amyloid oligomers. J Biol Chem 2005;280:17294–300
16. Pehar M, Vargas MR, Robinson KM, et al. Peroxynitrite transforms nerve growth factor into an apoptotic factor for motor neurons. Free Radic Biol Med 2006;41:1632–44
17. Lee R, Kermani P, Teng KK, et al. Regulation of cell survival by secreted proneurotrophins. Science 2001;294:1945–48
18. Backstrom JR, Miller CA, Tokes ZA. Characterization of neutral proteinases from Alzheimer-affected and control brain specimens: Identification of calcium-dependent metalloproteinases from the hippocampus. J Neurochem 1992;58:983–92
19. Lorenzl S, Albers DS, Relkin N, et al. Increased plasma levels of matrix metalloproteinase-9 in patients with Alzheimer's disease. Neurochem Int 2003;43:191–96
20. Gu Z, Kaul M, Yan B, et al. S-nitrosylation of matrix metalloproteinases: Signaling pathway to neuronal cell death. Science 2002;297:1186–90
21. Walker DG, Link J, Lue LF, et al. Gene expression changes by amyloid beta peptide-stimulated human postmortem brain microglia identify activation of multiple inflammatory processes. J Leukoc Biol 2006;79: 596–610
22. McGeer PL, McGeer EG. The inflammatory response system of brain: Implications for therapy of Alzheimer and other neurodegenerative diseases. Brain Res Brain Res Rev 1995;21:195–218
23. Smith MA, Perry G, Richey PL, et al. Oxidative damage in Alzheimer's. Nature 1996;382:120–21
24. Luth HJ, Holzer M, Gartner U, et al. Expression of endothelial and inducible NOS-isoforms is increased in Alzheimer's disease, in APP23 transgenic mice and after experimental brain lesion in rat: Evidence for an induction by amyloid pathology. Brain Res 2001;913:57–67
25. Luth HJ, Munch G, Arendt T. Aberrant expression of NOS isoforms in Alzheimer's disease is structurally related to nitrotyrosine formation. Brain Res 2002;953:135–43
26. Nguyen VT, Walker WS, Benveniste EN. Post-transcriptional inhibition of CD40 gene expression in microglia by transforming growth factor-beta. Eur J Immunol 1998;28:2537–48
27. Tan J, Town T, Paris D, et al. Microglial activation resulting from CD40-CD40L interaction after beta-amyloid stimulation. Science 1999; 286:2352–55
28. Calingasan NY, Erdely HA, Altar CA. Identification of CD40 ligand in Alzheimer's disease and in animal models of Alzheimer's disease and brain injury. Neurobiol Aging 2002;23:31–39
29. Togo T, Akiyama H, Kondo H, et al. Expression of CD40 in the brain of Alzheimer's disease and other neurological diseases. Brain Res 2000; 885:117–21
30. Lue LF, Kuo YM, Roher AE, et al. Soluble amyloid beta peptide concentration as a predictor of synaptic change in Alzheimer's disease. Am J Pathol 1999;155:853–62
31. McLean CA, Cherny RA, Fraser FW, et al. Soluble pool of Abeta amyloid as a determinant of severity of neurodegeneration in Alzheimer's disease. Ann Neurol 1999;46:860–66
32. Naslund J, Haroutunian V, Mohs R, et al. Correlation between elevated levels of amyloid beta-peptide in the brain and cognitive decline. JAMA 2000;283:1571–77
33. Walsh DM, Selkoe DJ. A beta oligomers—A decade of discovery. J Neurochem 2007;101:1172–84
34. Kayed R, Head E, Thompson JL, et al. Common structure of soluble amyloid oligomers implies common mechanism of pathogenesis. Science 2003;300:486–89
35. Familian A, Eikelenboom P, Veerhuis R. Minocycline does not affect amyloid beta phagocytosis by human microglial cells. Neurosci Lett 2007;416:87–91
36. Amin AR, Attur MG, Thakker GD, et al. A novel mechanism of action of tetracyclines: Effects on nitric oxide synthases. Proc Natl Acad Sci U S A 1996;93:14014–19
37. Ryu JK, Franciosi S, Sattayaprasert P, et al. Minocycline inhibits neuronal death and glial activation induced by beta-amyloid peptide in rat hippocampus. Glia 2004;48:85–90
38. Hensley K, Maidt ML, Yu Z, et al. Electrochemical analysis of protein nitrotyrosine and dityrosine in the Alzheimer brain indicates region-specific accumulation. J Neurosci 1998;18:8126–32
39. Smith MA, Richey Harris PL, et al. Widespread peroxynitrite-mediated damage in Alzheimer's disease. J Neurosci 1997;17:2653–57
40. Bruno MA, Clarke PB, Seltzer A, et al. Long-lasting rescue of age-associated deficits in cognition and the CNS cholinergic phenotype by a partial agonist peptidomimetic ligand of TrkA. J Neurosci 2004;24: 8009–18
41. Cleary JP, Walsh DM, Hofmeister JJ, et al. Natural oligomers of the amyloid-beta protein specifically disrupt cognitive function. Nat Neurosci 2005;8:79–84
42. Lesne S, Koh MT, Kotilinek L, et al. A specific amyloid-beta protein assembly in the brain impairs memory. Nature 2006;440:352–57
43. Stepanichev MY, Moiseeva YV, Lazareva NA, et al. Single intracerebroventricular administration of amyloid-beta (25–35) peptide induces impairment in short-term rather than long-term memory in rats. Brain Res Bull 2003;61:197–205
44. Olariu A, Tran MH, Yamada K, et al. Memory deficits and increased emotionality induced by beta-amyloid (25–35) are correlated with the reduced acetylcholine release and altered phorbol dibutyrate binding in the hippocampus. J Neural Transm 2001;108:1065–79
45. Tran MH, Yamada K, Olariu A, et al. Amyloid beta-peptide induces nitric oxide production in rat hippocampus: Association with cholinergic dysfunction and amelioration by inducible nitric oxide synthase inhibitors. FASEB J 2001;15:1407–9
46. Castegna A, Thongboonkerd V, Klein JB, et al. Proteomic identification of nitrated proteins in Alzheimer's disease brain. J Neurochem 2003;85: 1394–1401
47. Torreilles F, Salman-Tabcheh S, Guerin M, et al. Neurodegenerative disorders: The role of peroxynitrite. Brain Res Brain Res Rev 1999;30: 153–63
48. Xie Z, Wei M, Morgan TE, et al. Peroxynitrite mediates neurotoxicity of amyloid beta-peptide1–42- and lipopolysaccharide-activated microglia. J Neurosci 2002;22:3484–92
49. Dringen R. Oxidative and antioxidative potential of brain microglial cells. Antioxid Redox Signal 2005;7:1223–33
50. Li J, Baud O, Vartanian T, et al. Peroxynitrite generated by inducible nitric oxide synthase and NADPH oxidase mediates microglial toxicity to oligodendrocytes. Proc Natl Acad Sci U S A 2005;102: 9936–41
51. Wang Q, Rowan MJ, Anwyl R. Beta-amyloid–mediated inhibition of NMDA receptor–dependent long-term potentiation induction involves

activation of microglia and stimulation of inducible nitric oxide synthase and superoxide. J Neurosci 2004;24:6049–56
52. Alvarez B, Radi R. Peroxynitrite reactivity with amino acids and proteins. Amino Acids 2003;25:295–311
53. Heneka MT, Feinstein DL. Expression and function of inducible nitric oxide synthase in neurons. J Neuroimmunol 2001;114:8–18
54. Domeniconi M, Hempstead BL, Chao MV. Pro-NGF secreted by astrocytes promotes motor neuron cell death. Mol Cell Neurosci 2007; 34:271–79
55. Volosin M, Song W, Almeida RD, et al. Interaction of survival and death signaling in basal forebrain neurons: Roles of neurotrophins and proneurotrophins. J Neurosci 2006;26:7756–66
56. Figueiredo BC, Skup M, Bedard AM, et al. Differential expression of p140trk, p75NGFR and growth-associated phosphoprotein-43 genes in nucleus basalis magnocellularis, thalamus and adjacent cortex following neocortical infarction and nerve growth factor treatment. Neuroscience 1995;68:29–45
57. Holtzman DM, Li Y, Parada LF, et al. p140trk mRNA marks NGF-responsive forebrain neurons: Evidence that trk gene expression is induced by NGF. Neuron 1992;9:465–78
58. Li Y, Holtzman DM, Kromer LF, et al. Regulation of TrkA and ChAT expression in developing rat basal forebrain: Evidence that both exogenous and endogenous NGF regulate differentiation of cholinergic neurons. J Neurosci 1995;15:2888–905

